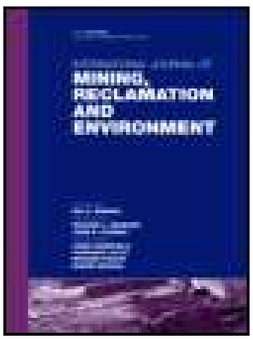

International Journal of Mining, Reclamation and Environment

ISSN: (Print) (Online) Journal homepage: https://www.tandfonline.com/loi/nsme20

Stochastic stope design optimisation under grade uncertainty and dynamic development costs

Matheus Furtado e Faria, Roussos Dimitrakopoulos & Cláudio Pinto

To cite this article: Matheus Furtado e Faria, Roussos Dimitrakopoulos & Cláudio Pinto (2021): Stochastic stope design optimisation under grade uncertainty and dynamic development costs, International Journal of Mining, Reclamation and Environment, DOI: 10.1080/17480930.2021.1968707

To link to this article: https://doi.org/10.1080/17480930.2021.1968707

Published online: 21 Sep 2021.

INTERNATIONAL JOURNAL OF MINING, RECLAMATION AND ENVIRONMENT
https://doi.org/10.1080/17480930.2021.1968707

Taylor & Francis
Taylor & Francis Group

Stochastic stope design optimisation under grade uncertainty and dynamic development costs

Matheus Furtado e Faria[a], Roussos Dimitrakopoulos[a] and Cláudio Pinto[b]

[a]Cosmo – Stochastic Mine Planning Laboratory, Department of Mining and Materials Engineering, McGill University, Montreal, Canada; [b]Department of Mining Engineering, Universidade Federal De Minas Gerais, Belo Horizonte, Brazil

ABSTRACT

Stope design optimisation defines three-dimensional extraction volumes aiming to maximise cashflows, subject to geotechnical and operational constraints. Available stope layout methods are deterministic, failing to account for grade uncertainty and variability that affect stope locations and sizes, as well as value. A two-stage stochastic integer programming model for stope design optimisation is proposed, integrating grade uncertainty quantified through geostatistical simulations, level allocation, variable stope and pillar sizes for different geotechnical zones, and development costs. An application at an underground gold mine employing sublevel open stoping highlights the integration and management of grade uncertainty to define risk-resilient stope design.

ARTICLE HISTORY
Received 11 May 2021
Accepted 10 August 2021

KEYWORDS
Stope design optimisation; stochastic integer programming; underground mine planning; geological uncertainty

1. Introduction

Stope design optimisation consists of defining underground mineable volumes whose shapes and sizes are dictated by the chosen stoping underground mining method, the geotechnical properties of the rock masses, and grade distribution of the orebody from which economic material will be extracted in order to maximise undiscounted profit [1,2]. In the current industrial practice, underground mine planning follows a sequential framework. An optimised stope design is an input to the development network layout optimisation, which defines the topology of interconnected access routes, such as shafts, declines, drifts, and crosscuts. Subsequently, the stopes and network layout are inputs to the production scheduling optimisation step, which dictates the underground mining project's net present value [3–8]. Grade uncertainty is the main contributor of technical risk, affecting a mining projects' viability [9,10]. However, it is not included in the conventionally generated stope designs, which fail to integrate the geological uncertainty and variability that affect stope sizes and locations, harming production and financial forecasts [11–14]. Therefore, the incorporation of supply uncertainty, in grade and material type, into the stope design optimisation allows one to address risk earlier in the planning process [5].

The sublevel open stoping is a self-supported and non-entry underground mining method, presenting some degree of selectivity and flexibility, in which the orebody is vertically split into production levels that are often separated by horizontal pillars. Within the primary levels, stopes are usually delimited by rib and longitudinal pillars, while regularly spaced blasting drifts are developed, defining the sublevels (Figure 1). The stopes remain empty during their exploitation with eventual post-backfilling [15–18]. Some three-dimensional sublevel stoping design optimisation

CONTACT Matheus Furtado e Faria matheus.faria@mail.mcgill.ca Cosmo – Stochastic Mine Planning Laboratory, Department of Mining and Materials Engineering, McGill University, Montreal, Canada

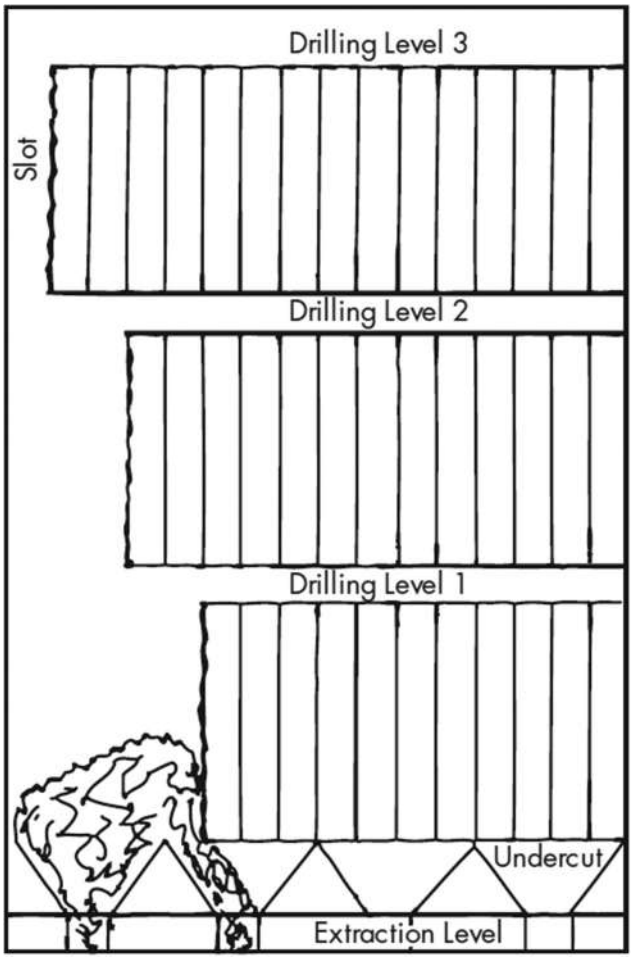

Figure 1. Stope in a sublevel stoping method, showing the sublevels and the typical parallel drilling ring pattern (Source: Bullock and Hustrulid 2001).

methods have been proposed, which incorporate progressively different geotechnical and operational aspects. The Floating Stope algorithm [19] and the Maximum Value Neighbourhood algorithm [20] float a fixed minimum stope size on the input orebody model and define profitable envelopes in which the stopes should be further manually designed. A predefined cut-off grade or the economic value of a block's neighbourhood is the respective criteria used to build the profitable boundaries in those methods. Topal and Sens [1] and Sandanayake et al. [21,22] present different methods to select non-overlapping stopes with variable sizes to define a stope layout with unified stopes. Furthermore, Sandanayake et al. [21,22] integrate more operational constraints, such as pillar requirements and level allocation.

The heuristic method proposed by Villalba Matamoros and Kumral [23] maximises the profit from stopes, which are defined by grouping slices of a fixed number of blocks in height and width and variable length, while minimising the internal dilution, which consists of slices with a grade that is lower than a specified cut-off grade. The previous methods are based on rectangular three-dimensional stope shapes. A heuristic approach combining a one-dimensional dynamic programming algorithm and dimensionality reduction greedy algorithm is proposed by Nikbin et al. [24] and generates stope boundaries with higher economic values compared to [19] and [20]. The stope overlapping issue and pillar constraints are further

integrated by [25]. The Mineable Shape Optimiser (MSO) [26–27] is an industry-standard software for stope design optimisation. In its Slice Method, the input model is discretized into a regular grid parallel to the main direction, forming transversal tubes. Each tube is sliced and the slices with grades greater than a specified cut-off grade are grouped to maximise each tube's economic value. However, this method is highly dependent on geological control parameters or wireframes, which are uncertain, and requires an upfront cut-off grade that is not adequately known in the early stages of the underground mine planning process. For a comprehensive review of stope design optimisation methods, the reader is directed to [2,5,28].

Some approaches aim to consider the development costs in the stope design optimisation, integrating the inherent interdependencies between each stope's economic potential and its accessibility/remoteness. The network flow-based method proposed by Bai et al. [29] imposes a maximum allowable distance of a block from a central shaft and requires a horizontal mining width for the accessibility of the farthest blocks in the output stope boundary. Ding et al. [30] propose an iterative approach that redistributes the development costs among selected stopes, re-evaluating their economic value. Hou et al. [31] implement a mixed-integer programming (MIP) formulation with recursive development cost constraints, which maximises the stopes' profit and minimises the total development costs for a fixed-network underground mine. However, the two last approaches are based on a development network layout with fixed shaft location and predefined levels, which have no flexibility to provide optimised production levels.

The previous methods are deterministic and are based on a single conventionally estimated orebody model, a smooth representation of the mineral deposit [32,33]. Geostatistically simulated representations of mineral deposits better represent grade and material-type distributions of a deposit, reproducing conditional data statistics and are used to quantify the grade uncertainty and variability [32,34]. Some stochastic stope design optimisation methods have been proposed. Grieco and Dimitrakopoulos [35] present a probabilistic mathematical programming formulation with flexible pillar requirements tailored to the sublevel stoping method. Stochastic simulations of a deposit, discretized into blasting rings, are used to derive the ring's average grade and its probability of being above a predefined cut-off grade. The model aims to maximise the stope design's metal content, given a minimum acceptable risk level. The probabilistic approach, however, uses limited information consisting of summarised probabilities representing the uncertainty and estimated grades. Thus, simulations are not directly integrated. Villalba Matamoros and Kumral [36] propose a three-step stochastic stope design optimisation method for a non-specified stoping method variant. First, the previously mentioned heuristic algorithm of [23] generates a stope design for each input simulation. Subsequently, the designs are clustered based on their similarities while fixing geotechnical constraints violations to obtain a population of risk-resilient designs. Finally, a genetic algorithm combines the resulting designs to maximise the profit and ensure the single final design's feasibility. The previously discussed stochastic approaches do not propose scenario-dependent recourse actions, preventing the methods from adapting to grade uncertainty.

Two-stage stochastic integer programming (SIP) formulations [37] were initially introduced in mine planning for long-term production scheduling of a single open-pit mine [38,39] and have since been successfully extended to the simultaneous optimisation of mining complexes [40–43]. Although fewer applications have been applied to underground settings, recent promising SIP formulations have been developed for long-term underground mine production scheduling employing different mining methods, such as a hybrid cut-and-fill with long-hole [44], purely cut-and-fill [45], and block caving [46]. The applications demonstrate that the stochastic frameworks capitalise on the grade and operational uncertainties to provide physically different schedules with a higher expected net present value, while managing the risk of not achieving production targets when compared to the deterministic approaches.

Unlike the vast majority of available methods, which only aim to maximise the undiscounted profit or recovered metal, a new two-stage SIP formulation for stope design optimisation is proposed in this paper. Its objectives are to maximise the undiscounted profit whilst minimising related development

costs, and the economic impact of exceeding project capacities. The risk management is incorporated through scenario-dependent recourse actions given the set of geostatistical simulations of the related orebody. The proposed first-stage decisions account for the physical constraints to provide a unique and mineable sublevel stoping design, which are related to selecting levels, stopes, the location of a main shaft, and the horizontal and vertical development costs associated with opening drifts and the shaft, respectively. The second-stage decisions aim to maximise the recovered metal while managing the risk of not satisfying existing or planned capacities under the grade uncertainty. The model inputs the realisations of the deposit, which has blocks that are flagged with distinct geotechnical zones, a set of potential primary access options, such as different shaft locations, the economic and technical parameters, and a library defining the level spacing, the possible stope shapes and pillar sizes for each geotechnical zone. The output is a stope layout with the best levels and stopes locations, as well as the best shaft location that minimise the development costs of shaft and drifts. The next sections discuss an overview of the method, followed by the two-stage SIP formulation. Subsequently, a case study at an underground gold mine is presented and benchmarked with the stope layout generated by an industry-standard stope design approach. Conclusions and future work follow.

2. Method

A proposed stochastic stope design optimisation method under grade uncertainty and development costs is presented. The sublevel open stoping mining method (Figure 1) considers horizontal production levels that might be separated by horizontal pillars. The stopes have variable heights within each level, but their access is always aligned to a respective production level and can be apart by rib and longitudinal pillars. This feature facilitates the mineability of the stope layout and the optimisation of the detailed development design of hauling and drilling drifts and loading crosscuts connecting the selected stopes in the further steps of the underground mine planning.

This section introduces the required inputs, and the preprocessing steps are discussed, followed by the two-stage SIP's mathematical formulation. The proposed method receives a set of stochastic orebody simulations $s \in S$, which quantify the geological uncertainty and variability in grades and material types of mining blocks $i \in I$. The blocks are flagged with different input geotechnical zones $n \in N$ with respective stope size and pillars requirements. A set of potential access options, such as different shaft locations, and relevant economic and geotechnical parameters complete the required inputs. The following tables include the definitions and the notation used to specify the proposed SIP model, such as the list of indices (Table 1) and sets (Table 2), the economic and technical parameters (Table 3), the geometric parameters related to the underground mining method considered (Table 4), as well as the binary (Table 5) and fractional (Table 6) decision variables that control the proposed stope design optimization framework., , $k \in K$

2.1. Stopes and levels preprocessing steps

The proposed approach follows the steps presented in Figure 2, which provide a set L of possible levels, with related sets Ω_l and Λ_l of overlapping and adjacent levels, and potential stopes within each level J_l, with associated sets Ω_{jl} and Λ_{jl} of overlapping and adjacent stopes. The steps will be presented in detail in the following subsections.

2.1.1. Level splitting

First, the set of blocks $i \in I_n$ belonging to a defined geotechnical zone $n \in N$ is vertically split, from bottom to top, into a set of layers of blocks whose height (in terms of numbers of blocks along the vertical coordinate) corresponds to the set up level spacing $\alpha_n^{\mathbf{z}}$ of zone n. A generated layer of blocks will be a potential production. Once the top of the block model is reached, the level splitting restarts by skipping some blocks in the bottom of the geotechnical zone based on the shift parameter $\beta_n^{\mathbf{z}}$. In

Table 1. List of sets.

Set	Definition
I	Set of blocks i in the entire orebody model
I_n	Set of blocks i in zone n
I_l	Set of blocks i in level l
I_{jl}	Set of blocks i in stope j of level l
J	Set of all potential stopes j
J_l	Set of potential stopes j in a level l
J_{dlk}	Set of potential stopes in mining direction d in level l for access option k
N	Set of disjoint geotechnical zones n
L	Set of all possible levels l
L_n	Set of potential levels l of geotechnical zone n
S	Set of geological uncertainty scenarios s
K	Set of access options k
Ω_l	Set of levels l' that overlap with level l, such that $l, l' \in L_n$ and $n \in N$
Ω_{jl}	Set of stopes j' that overlap with stope j, such that $j.j' \in J_l$, in level $l \in L_n$, $n \in N$
Λ_l	Set of levels l' of other geotechnical zones that are adjacent to level $l \in L_n$ such that $l' \in \Lambda_l \subset L \backslash L_n$
Λ_{jl}	Set of stopes j' in levels $l' \in \Lambda_l$ that overlap with stope $j \in J_l$ in level$l \in L_n$
D_l	Set of mining directions d in level l
M_n	Set of stope shapes m of geotechnical zone $n \in N$

Table 2. List of economic and technical parameters.

Parameter	Definition
w_{is}	Tonnage of block i in scenario s
w_{jls}	Tonnage of stope j in level l, $w_{jls} = \sum_{i} w_{is}$ in scenario s
θ_{is}	Indicator $\theta_{is} = 1$ if block i is greater than a user-defined cut-off grade is scenario s, 0 otherwise.
o_{jls}	Ore tonnage of stope j in level l and scenario s, $o_{jls} = \sum_{i \in I_{jl}} \theta_{is} w_{is}$
g_{is}	Grade of block i in scenario s in percent metal
g_{jls}	Average grade of ore blocks within stope j in level l scenario s in percent metal, such that $g_{jls} = \sum_{i \in I_{jl}} \theta_{is} g_{is} w_i / o_{jls}$.
R	Processing recovery in percent
P	Metal selling price \$/t
C_l^{drift}	Unit horizontal development cost of drifts in \$/m in level l
C_k^{shaft}	Unit vertical (shaft) development cost associated with access option $k \in K$ in \$/m.
C_l^{mining}	Mining cost in \$/t for level l.
$C^{process}$	Processing cost in \$/t.
$U_k^{transport}$	Total transportation (hoisting) capacities of access options $k \in K$ in tons.
$U^{develop}$	Total horizontal development capacity in m.
U^{mill}	Total milling capacity in tons
$c^{transport}$	Penalty cost associated with the surplus deviations from the transportation (shaft or ramp) capacity.
$c^{develop}$	Penalty cost associated with the surplus deviations from the horizontal development capacity.
$c^{process}$	Penalty costs associated with the surplus deviations from the mill tonnage capacity.
c^{metal}	Penalty cost associated with the shortages from the metal content of the stopes selected in a level compared to the metal content of all blocks $i \in I_l$ (applied to each level l

the end of this process a set of overlapping potential levels $l \in L_n$ is generated as depicted in Figure 3. The total set potential levels is defined as the union of levels of all geotechnical zones, that is, $L = U\, n \in N L_n$. The distances δ_{lk}^{shaft} (Figure 4) from the surface to levels l along each access option $k \in K$ are determined based on the coordinates of the surface $z_k^{surface}$ and the base of each level $\mathbf{z}_l^{base}$. It is assumed that the generated levels are formed by blocks belonging to a unique geotechnical zone.

2.1.2. Level overlapping search

The generated levels overlap with some other levels since they share some layers of blocks. Furthermore, due to geotechnical requirements, a horizontal (sill/crown) pillar with a minimum height $\sigma_n^{sill,\mathbf{z}}$ (in terms of the number of blocks in $\mathbf{z}$ axis) should be ensured between two selected levels in the output design within each zone n. Therefore, the overlaps between levels are mapped

Table 3. List of geometric parameters.

Parameter	Definition
x_i, y_i, z_i	Coordinates of block i in metres
$\lambda^x, \lambda^y, \lambda^z$	Block dimensions in metres
θ_j	Origin block of stope j with coordinates $x_{\theta_j}, y_{\theta_j}, z_{\theta_j}$
e_j	Terminal block of stope j with coordinates $x_{e_j}, y_{e_j}, z_{e_j}$
$Y^x_{mn}, Y^y_{mn}, Y^z_{mn}$	Stope sizes along direction x, y, and z in number of blocks for stope shape $m \in M_n$ of geotechnical zone $n \in N$
α^z_n	Fixed level height, in terms of the number of blocks, along z axis for geotechnical zone $n \in N$
β^z_n	Shift parameter corresponding to the number of blocks to be shifted above the base coordinates z_1^{base} of the most profound level $l = 1$ of zone n, such that $\beta^z_n < \alpha^z_n$
z_l^{base}	Coordinate of the base of level l
z_l^{roof}	Coordinate of the roof of level l
$z^{surface}$	Coordinate of surface (starting point of shaft/ramp).
$\sigma_n^{rib,x}$	Minimum stand-off pillar size between stopes along axis x in metres for geotechnical zone $n \in N$ (multiple of dimension λ^x)
$\sigma_n^{rib,y}$	Minimum stand-off pillar size between stopes along axis y in metres for geotechnical zone $n \in N$ (multiple of dimension λ^y)
$\sigma_n^{sill,z}$	Minimum pillar size in number of blocks between levels along axis z in metres for geotechnical zone $n \in N$ (multiple of dimension λ^z)
δ_{lk}^{shaft}	Vertical distance from the surface to z_l^{base} of level l for access option $k \in K$ (shaft)
δ_{jdlk}^{drift}	Horizontal distance (in a drift) from stope j to a potential access point of option $k \in K$ along mining direction d in level l

Table 4. Binary decision variables.

Variable	Definition
y_{jl}	Stope selection decision variable, equal to 1 if stope j in level l is selected, and 0 otherwise
z_{lk}	Level selection decision variable, equal to 1 if level l is selected under access option k, and 0 otherwise
ω_k	Access option selection decision variable, equal to 1 if option k is selected, and 0 otherwise

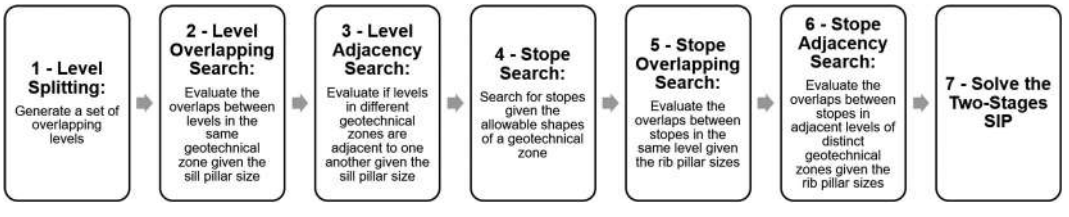

Figure 2. Steps of the proposed stochastic stope design optimisation.

based on their relative base and roof coordinates, $\mathbf{z}_l^{base}$ and $\mathbf{z}_l^{roof}$, respectively, and the parameter $\sigma_n^{sill,\mathbf{z}}$ as presented in Figure 5a. For instance, levels l and l', such that $l, l' \in L_n$, overlap with each other if $\mathbf{z}_l^{base} \leq \mathbf{z}_{l'}^{base}$ and $\left(\mathbf{z}_l^{roof} + \sigma_n^{sill,\mathbf{z}}\right) \leq \mathbf{z}_{l'}^{base}$ or if $\mathbf{z}_{l'}^{base} \leq \mathbf{z}_l^{base}$ and $\mathbf{z}_{l'}^{roof} \leq \left(\mathbf{z}_l^{base} - \sigma_n^{sill,\mathbf{z}}\right)$. The level overlapping search generates a set of levels $l' \in \Omega_l$ that overlap with level $l \in L_n$.

2.1.3. Level adjacency search

Depending on the modelled surfaces' spatial configuration that individualises geotechnical zones, two distinct zones n and n' might coexist for some $\mathbf{z}$ coordinates. Therefore, some levels of their correspondent sets L_n and $L_{n'}$ might be adjacent. The level adjacency search (Figure 5b) follows the

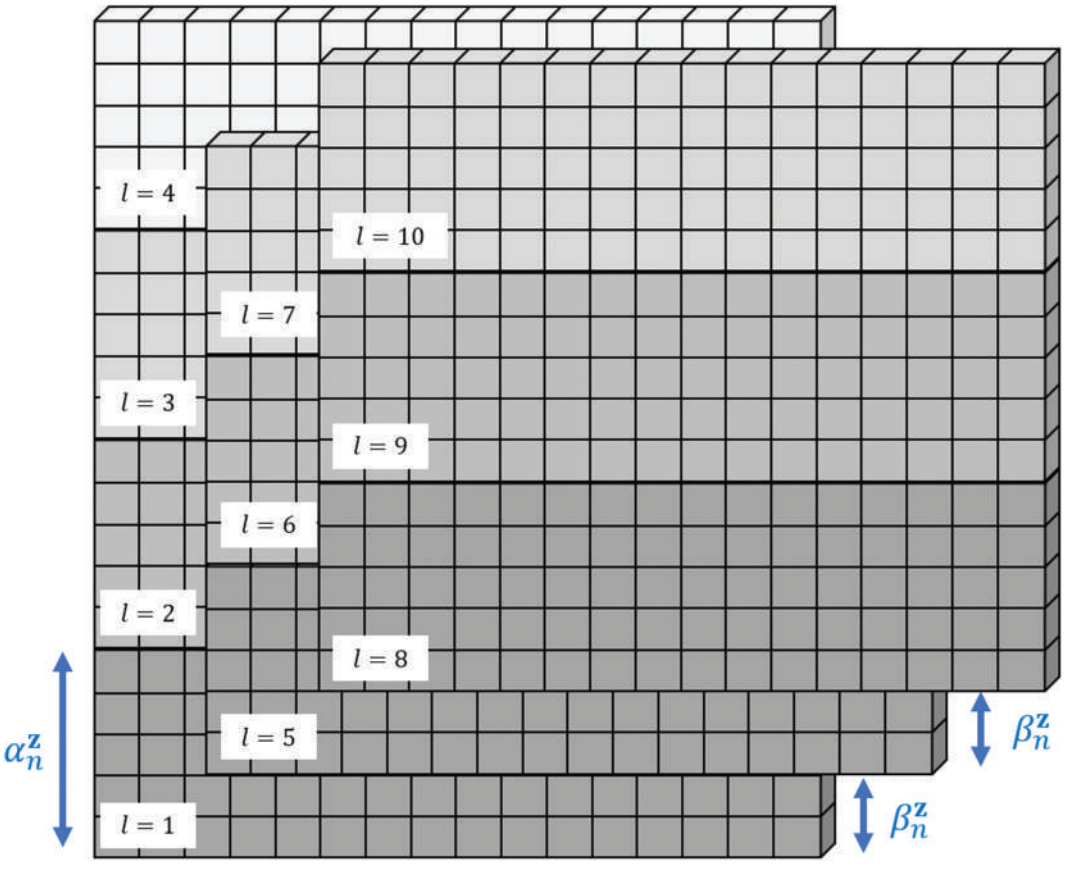

Figure 3. Representation of the level splitting step generating the set of levels L_n of geotechnical domain n.

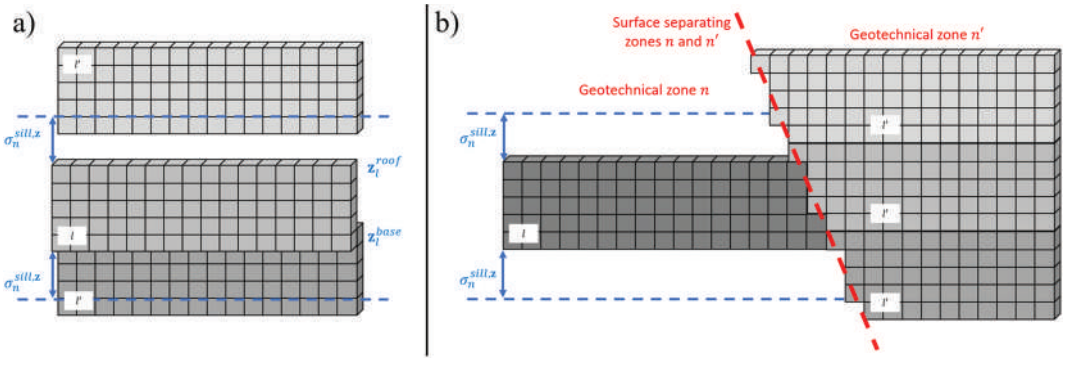

Figure 4. Parametrised distances (in red) considered by the method for an access option k, a potential level l, two mining directions d and d' and two potential stopes j and j'.

same conditions mentioned above of the level overlapping search step (Figure 5a). In this instance, the adjacency occurs between levels in distinct zones, i.e. $l \in L_n$ and $l' \in L_{n'} \subset L \backslash L_n$, and generates the subset of levels $l' \in \Lambda_l$ that are adjacent to level l.

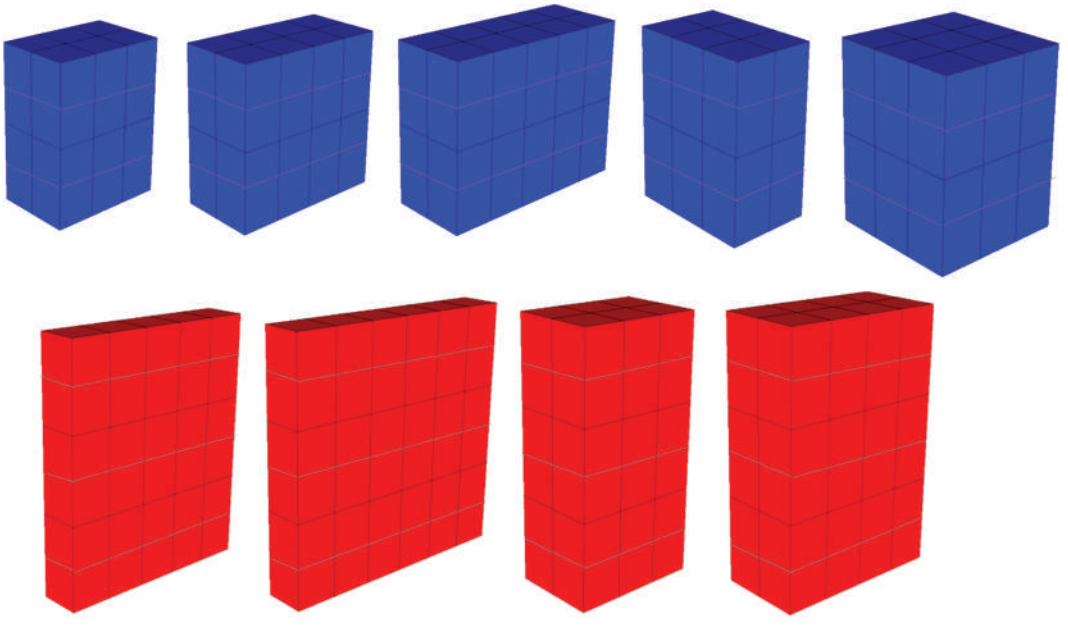

Figure 5. A) Representation of the level overlapping search, and b) the level adjacency search.

2.1.4. Stope search

A library of potential stope shapes is defined for each geotechnical domain $n \in N$ (Figure 6). Each shape $m \in M_n$ consists of the number of blocks γ^{x}_{mn}, γ^{y}_{mn} and γ^{z}_{mn} along axes **x**, **y** and **z**. A broad combination of stope shapes improves the output stope design since the optimisation process has more flexibility to select potential stopes and may better control dilution. However, geotechnical considerations, due to required stope's size and shape relationships for stable openings [16,47,48], may limit the possible combinations of stope shapes in terms of number of blocks per stope.

Given the dimensions γ^{x}_{mn}, γ^{y}_{mn} and γ^{z}_{mn}, the stope shapes $m \in M_n$ are floated within each of generated layers of mining blocks forming the potential levels $l \in L_n$. This step produces the set of overlapping potential stopes J_l within a level $l \in L_n$. It is assumed that all stopes must lie at the base of their level. Therefore, the stope search step looks for stopes with origin block θ_j coinciding with the bottom of the respective potential level. Once a stope is defined, it is identified by its index $j \in J_l$ and its starting and ending blocks, respectively, θ_j and e_j (Figure 7a). During the current step, the stope economic values v_{jls} for each simulation $s \in S$ are computed. The stopes whose probability of negative economic value is higher than a threshold [49] can be eliminated. Finally, depending on the relative position to an access option k, the stopes are flagged to a mining direction$d \in D_l$, for example, the eastern and western sides of a shaft along the strike, forming the subsets of stopes J_{dlk}. Furthermore, the approximated drift development distances δ^{drift}_{jdlk} along the specified mining directions are computed, allowing assessment of the accessibility of a stope (Figure 4).

2.1.5. Stope overlapping search

The proposed method assumes that the generated stope design must satisfy operational and geotechnical constraints in order to be readily used as an input for the subsequent optimisation of long-term mine production scheduling [7,8,50,51]. Non-overlapping constraints for stopes avoid the manual post-treatment of a stope boundary with overlapping stopes required by some related methods [19,20,24,25,29]. Furthermore, due to stability considerations, longitudinal and

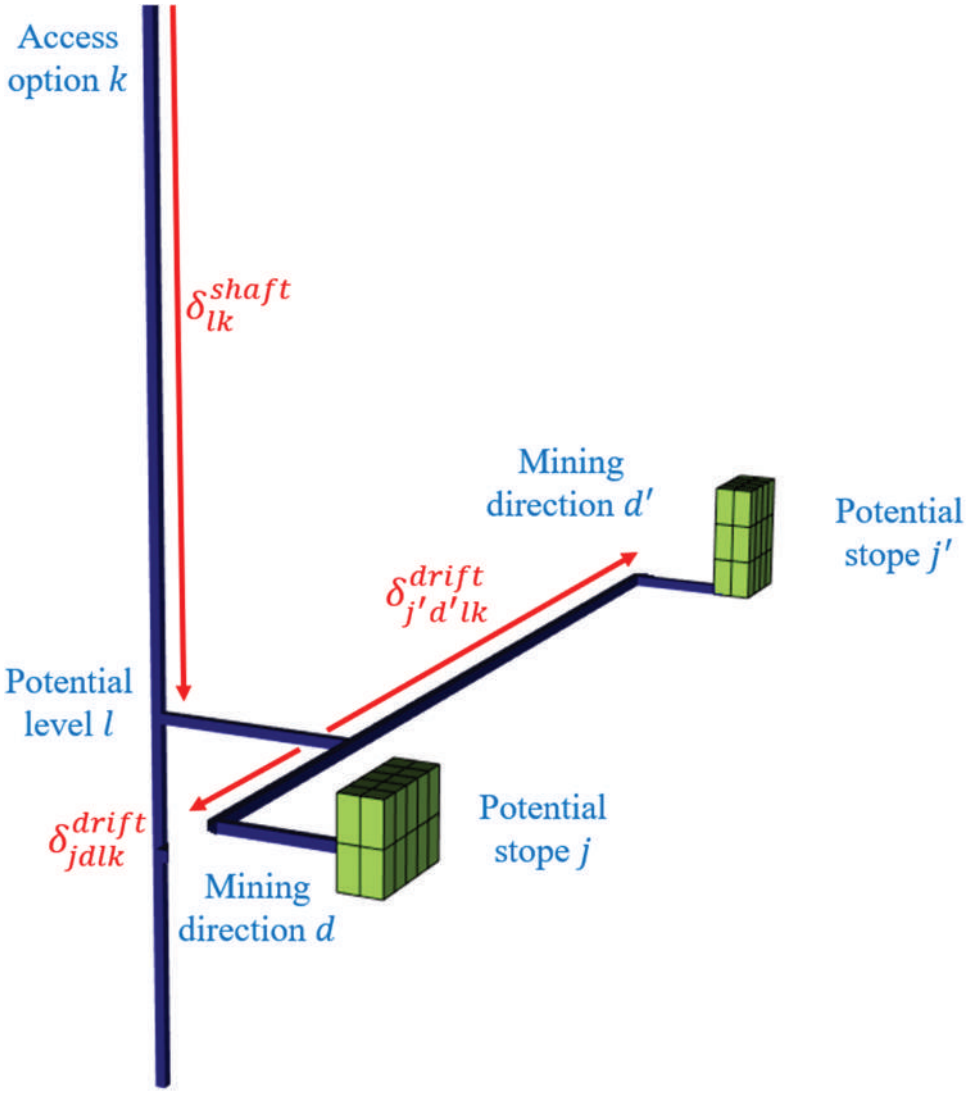

Figure 6. Allowable stope shapes for two geotechnical zones.

rib pillars must be placed between stopes. The stope overlapping search is performed based on the minimum pillar sizes, in terms of number of blocks, $\sigma_n^{rib,\mathbf{x}}$ and $\sigma_n^{rib,\mathbf{y}}$ along axes x and y for each zone $n \in N$. Henceforth, these pillars will be named indistinctly as rib pillars, although in the literature, rib pillars are usually transverse to the strike [16,17]. The stopes overlapping conditions are defined given the minimum pillar sizes and the coordinates of the starting θ_j and end e_j blocks of the stopes. As shown in Figure 7b, a stope j' and the reference stope j overlap with each other if $\mathbf{x}_{\theta_j} \leq \mathbf{x}_{\theta_{j'}}$ and $\left(\mathbf{x}_{e_j} + \sigma_n^{rib,\mathbf{x}}\right) \geq \mathbf{x}_{\theta_{j'}}$ or if $\mathbf{y}_{\theta_j} \leq \mathbf{y}_{\theta_{j'}}$ and $\left(\mathbf{y}_{e_j} + \sigma_n^{rib,\mathbf{y}}\right) \geq \mathbf{y}_{\theta_{j'}}$. The stope overlapping search, for each pair $j, j' \in J_l$ and $l \in L_n$, defines the set of stopes $j' \in \Omega_{jl}$ that overlap with j.

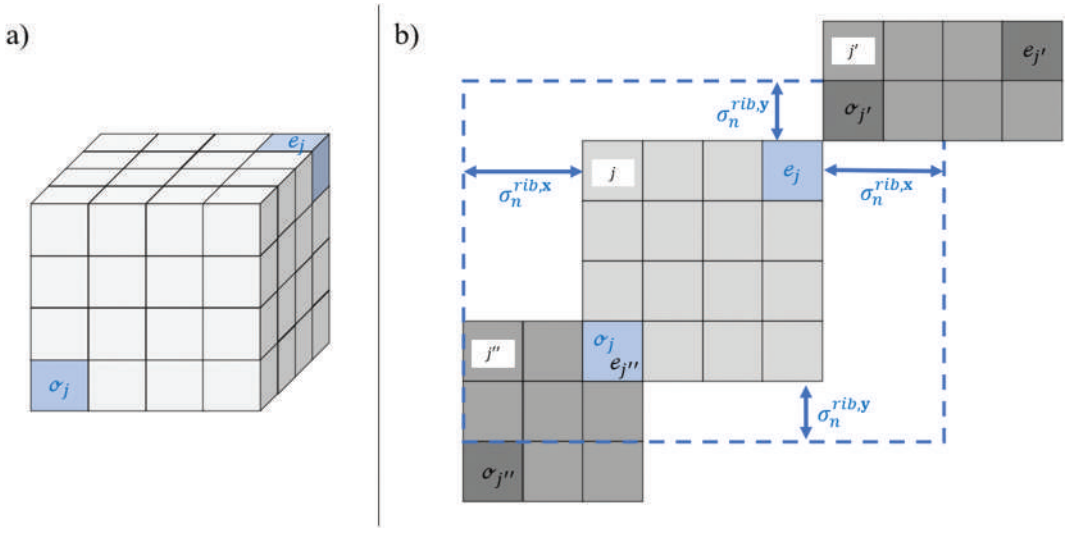

Figure 7. A) Representation of starting and ending blocks of a stope, and b) the stope overlapping search step in plan-view.

2.1.6. Stope adjacency search

Overlaps must also be avoided for stopes in different geotechnical domains if the current level l has a non-empty adjacency set, i.e. $\Lambda_l \neq \emptyset$ (Figure 5b). Therefore, a similar overlapping search (Figure 7b) is performed to define the set of stopes $j' \in \Lambda_{jl}$ that overlap with stope j, such that $j \in J_l$, $l \in L_n$ and $j' \in J_{l'}$, $l' \in \Lambda_l$.

2.2. Mathematical formulation

Three binary decision variables control the proposed stochastic stope design optimisation framework. The access options decision variables $\omega_k \in \{0,1\}$ control whether an access option $k \in K$ is selected or not for stope design. Level selection decision variables $z_{lk} \in \{0,1\}$ control which production levels $l \in L$ are selected for the final design given the decision of access option. The stope selection decision variables $y_{jl} \in \{0,1\}$ define whether a stope $j \in J_l$ in level $l \in L$ is to be extracted. The bold characters **y** and **z** refer to the coordinates of blocks, stopes, and levels, whereas the italic characters y and z are used for the decision variables present in the proposed stochastic mathematical programming formulation.

Two types of development costs are integrated into optimisation. The vertical development cost VDC_k stands for the excavation and commissioning costs associated with shaft option $k \in K$, while the horizontal development cost HDC_{dlk} relates to the excavation and commissioning of the haulage and drilling drifts to access the selected stopes in level $l \in L$ through mining direction $d \in D_l$. The total HDC_{lk} present in the objective function accounts for the contribution of the development costs overall directions $d \in D_k$.

2.2.1. Objective function

The proposed method aims to maximise the selected stopes' potential revenue while integrating other components in the objective function of Eq. 1. Part I of the objective function represents the maximisation of the economic value of the selected stopes. Part II accounts for the minimisation of the overall vertical development cost and the sum of the horizontal development costs of all possible levels given the access options $k \in K$. Part III penalises the resulting economic impact of exceeding the project capacities of transportation, the development of drifts, and processing. These overall capacities are defined based on each component's yearly capacity and an assumed life of mine

horizon for the project at hand. Part IV tries to extract the upside potential of the design given the grade uncertainty by penalising the economic difference $d_{ls}^{\$metal}$ related to the metal content of all blocks in a level $i \in I_l$ and the recoverable metal within the selected stopes in the design, that is, $j \in J_l$, for $l \in L$.

$$\max \underbrace{\frac{1}{|S|}\sum_{s\in S}\sum_{l\in L}\sum_{j\in J_l} v_{jls}y_{jl}}_{Part\,I:\,Revenue\,from\,each\,stope} \underbrace{-\sum_{k\in K}\left(VDC_k+\sum_{l\in L}HDC_{lk}\right)}_{Part\,II:\,Vertical\,and\,horizontal\,development\,costs} \underbrace{-\frac{1}{|S|}\sum_{s\in S}\left(c^{transport}d_s^{\$transport}+c^{develop}d^{\$develop}+c^{process}d_s^{\$process}\right)}_{Part\,III:\,Penalties\,applied\,to\,the\,entire\,stope\,design} \underbrace{-\frac{1}{|S|}\sum_{s\in S}\sum_{l\in L}c^{metal}d_{ls}^{\$metal}}_{Part\,IV:\,Penalties\,applied\,to\,each\,level} \quad (1)$$

The penalties costs $c^{transport}$, $c^{develop}$, $c^{process}$ and c^{metal} are set by a user-based empirical approach that generally relies on testing the order of magnitude for unit cost violations [38,39,52]. Acknowledging that an underground mining project is constrained by the overall capacities addressed in Part III and the miner planner's pre-emption to favour the upside potential of the design in Part IV, the objective function integrates this trade-off into the optimisation process to provide an optimal and uncertainty-based stope design.

The proposed method offers the possibility to use or not a cut-off grade. For a specified cut-off grade, the economic value v_{ils} of a block $i \in I_l$ in level $l \in L$ in simulation $s \in S$ is defined by Eq. 2. If a cut-off grade is not defined, Eq. 2 would have only its upper part. Since a mining block can belong to different potential levels $(i \in I_l)$, it has multiple economic values v_{ils}, for each level and simulation. In addition, level-based mining costs C_l^{mining} accounting for extraction, backfilling, and material handling might reflect increasing costs with depth.

$$v_{ils} = \begin{cases} w_{is}\left(g_{ils}RP - \left(C^{process} + C_l^{mining}\right)\right), g_{ils} \geq cut-off \\ -w_{is}C_l^{mining}, otherwise \end{cases} \quad (2)$$

The economic value of a stope v_{jls}, in turn, is determined by the sum of the economic values v_{ils} of all its blocks $(i \in I_{jl})$ and could also consider its horizontal distance from each access option. Note that Eq. 3 assigns higher costs for larger stopes. Considering a family of potential stopes that share a common high-grade block, the larger stopes centred in this block are likely to have more-low grade and waste blocks, resulting in a reduced value v_{jls}. Hence, the optimisation process would opt for a smaller stope containing this high-grade block. As a result, even though the current decision variables y_{jl} are in stope support scale, the family of potential stopes that share this high-grade block carries the information on a block basis, and consequently, the optimisation process is able to select the better stope locations and sizes in order to control dilution.

$$v_{jls} = \sum_{i\in I_{jl}} v_{ils} \quad (3)$$

2.2.2. Constraints

This section presents the constraints related to geotechnical requirements, the specified capacities, development costs, and link between different variables.

$$\sum_{k \in K} \omega_k = 1 \tag{4}$$

$$z_{lk} \leq \omega_k, \quad k \in K, l \in L \tag{5}$$

$$y_{jl} \leq \sum_{k \in K} z_{lk}, \quad l \in L, j \in J_l \tag{6}$$

$$z_{lk} + z_{l'k} \leq 1, \quad l' \in \Omega_l \subset L_n, l \in L_n \tag{7}$$

$$y_{jl} + y_{j'l} \leq 1, \quad j' \in \Omega_{jl}, j \in J_l, l \in L \tag{8}$$

$$y_{jl} + y_{j'l'} \leq 1, \quad j' \in \Lambda_{jl}, l' \in \Lambda_l \subset L \backslash L_n, j \in J_l, l \in L_n \tag{9}$$

Equation 4 ensures that only one access option is selected. The linking constraints of Eq. 5 state that a level l can be opened with access option k, only if this access option is selected, while Eq. 6 guarantees that a stope j can be selected if its level l is selected, and vice-versa. Two overlapping levels, including sill/crown pillar requirements, in a geotechnical zone $n \in N$ cannot be simultaneously selected in the design (Eq. 7) as well as two overlapping stopes, including rib pillar requirements, within the same level and geotechnical zone $l \in L_n$ (Eq. 8). The overlaps must also be avoided between the stopes in the contact between two adjacent levels in distinct geotechnical zones. Such type of overlaps is avoided Eq. 9.

$$VDC_k \geq \left(\delta_{lk}^{shaft} C_k^{shaft}\right) z_{lk}, \quad l \in L, k \in K \tag{10}$$

$$HDC_{dlk}^{'} \geq \left(\delta_{jdlk}^{drift} C_l^{drift}\right) y_{jl}, \quad j \in J_{dlk}, d \in D_l, l \in L, k \in K \tag{11}$$

$$HDC_{lk}^{'} \geq \sum_{d \in D_l} HDC_{dlk}^{'}, \quad l \in L, k \in K \tag{12}$$

$$HDC_{lk} \leq M\omega_k, \quad l \in L, k \in K \tag{13}$$

$$HDC_{lk} \leq HDC_{lk}^{'}, \quad l \in L, k \in K \tag{14}$$

$$HDC_{lk} \geq M(\omega_k - 1) + HDC_{lk}^{'}, \quad l \in L, k \in K \tag{15}$$

The integration of the development costs, a substantial proportion of a stope global cost, aims to address the interdependencies between the stope layout and the development network. The proposed approach has linear constraints that determine overall horizontal development cost per level and vertical development cost for the entire design. The vertical development cost for each access option $k \in K$ is determined by Eq. 10. The distance from the surface δ_{lk}^{shaft} and the respective unit cost C_k^{shaft} parametrise this cost. Whenever the activation of a variable z_{lk} opens a more profound level, the VDC_k is incremented, entailing in a higher overall cost for the stope design.

Similarly, in Eq. 11, the horizontal development cost for each potential level $l \in L$ and access option $k \in K$ along each mining direction $d \in D_l$ depends on the distance from a stope to an access option δ_{jlk}^{drift} and the unit drift development cost C_l^{drift}. The selection of a stope further from the access option in a direction d will raise the variable $HDC_{dlk}^{'}$. Therefore, this stope will be selected if it is sufficiently valuable to pay for this additional drift development, avoiding unreasonable costs. The overall drift development cost in a level $HDC_{lk}^{'}$ corresponds to the sum over all mining directions (Eq. 12). The

optimisation process balances the revenue from the selected stopes and the drifts development cost at a potential level. Equations 12–15 link the variables HDC'_{lk} with the access option decisions ω_k and are used to linearise the formulation by avoiding the product $HDC'_{lk}\omega_k$, which is replaced by a new variable HDC_{lk}. In Eqs. 13 and 15, $\mathcal{M} > 0$ is a sufficiently large constant that activates the constraint in the case $\omega_k = 1$ by imposing a loose upper bound on the horizontal development cost variable HDC_{lk}. Indeed, this last variable is minimised in the objective function (Eq. 1 – Part II).

$$\sum_{l\in L}\sum_{j\in J_l}\left(y_{jl}w_{jls}\right) - d_s^{transport} \leq \sum_{k\in K} U_k^{transport}\omega_k, \quad s \in S \tag{16}$$

$$\sum_{l\in L}\sum_{k\in K}\left(\frac{HDC_{lk}}{DC}\right) - d^{develop} \leq U^{develop} \tag{17}$$

$$\sum_{l\in L}\sum_{j\in J_l}\left(y_{jl}o_{jls}\right) - d_s^{process} \leq U^{process}, \quad s \in S \tag{18}$$

Some existing or planned capacities might constrain the underground mining project. Therefore, some overall capacities defined by yearly capacities and the projected life-of-mine are considered in these constraints. The surplus deviations $d_s^{transport}$, $d^{develop}$ and $d_s^{process}$ from the specified capacities are defined in Eqs. 16–18. Equation 16 defines the overall transportation capacity in tons $U_k^{transport}$ of the selected access option $k \in K$. The development advancement of drifts might also be constrained, and its overall capacity $U^{develop}$ in metres is ensured in Eq. 17, where the ratio HDC_{lk}/DC reflects the maximum distance to be developed per level assuming access option $k \in K$. The overall processing capacity $U^{process}$ must be satisfied considering the sum of the contained ore tonnage o_{jls} in simulation $s \in S$ (Eq. 18).

$$\underbrace{\sum_{i\in I_l}\left(w_i\theta_{ils}g_{ils}\right)}_{\substack{maximummetal\\ contentinlevell}} - \underbrace{\sum_{j\in J_l}\left(o_{jls}g_{jls}y_{jl}\right)}_{\substack{metalcontentinthe\\ selectedstopesinlevell}} - d_{ls}^{metal} \leq 0, \quad l \in L, s \in S \tag{19}$$

Aiming to capture the upside potential of recoverable metal in the stope design given the geological uncertainty, Eq. 19 penalises the reduction in metal content of the stope design in level $l \in L$ compared to the total metal content in that level. Levels that have more potential for profitable stopes are less penalised, as well as the levels that have minor variations in metal content, that is d_{ls}^{metal}, among all simulations. Part IV of the objective function acts by maximising the metal content of the stope design under uncertainty and translates the mine planer's tendency to foresee the potential stoping areas translated by the magnitude of the penalty c^{metal}.

$$d_s^{\$transport} = C_l^{mining} d_s^{transport}, \quad s \in S \tag{20}$$

$$d^{\$develop} = C_l^{drifts} d^{develop} \tag{21}$$

$$d_s^{\$process} = C^{process} d_s^{process}, \quad s \in S \tag{22}$$

$$d_{ls}^{\$metal} = P d^{metal}, \quad l \in L, s \in S \tag{23}$$

The previously defined deviations have a different order of magnitude. For instance, $d_s^{transport}$ and $d_s^{process}$ are defined in terms of tonnage of material mined and processed, $d^{develop}$ in metres of development and d_{ls}^{metal} in metal tonnage. Therefore, in Eqs. 20–23, the initial deviations are

multiplied by pertinent unit costs, or the metal price, converting them into dollar value deviations, with superscript $. These equations provide a balance between the different components of the objective function that drives the optimisation process. Finally, the integrality and non-negativity constraints from Eq. 24 to Eq. 32 complete the SIP formulation and are as follows:

$$y_{jl} \in \{0,1\}, \quad j \in J_l, l \in L \tag{24}$$

$$z_{lk} \in \{0,1\}, \quad l \in L, k \in K \tag{25}$$

$$\omega_k \in \{0,1\}, \quad k \in K \tag{26}$$

$$VDC_k \geq 0, \quad k \in K \tag{27}$$

$$HDC_{lk}, HDC'_{lk} \geq 0, \quad l \in L, k \in K \tag{28}$$

$$HC'_{dlk} \geq 0, \quad d \in D_l, l \in L, k \in K \tag{29}$$

$$d_s^{transport}, d_s^{\$transport}, d_s^{process}, d_s^{\$process} \geq 0, \quad s \in S \tag{30}$$

$$d^{develop}, d^{\$develop} \geq 0 \tag{31}$$

$$d_{ls}^{metal}, d_{ls}^{\$metal} \geq 0, \quad l \in L, s \in S \tag{32}$$

3. Case study – Application at an underground gold mine

In this section, the proposed stochastic stope design optimisation, under grade uncertainty and considering development costs, is applied to an underground gold deposit employing the sublevel open stoping mining method. The uncertainty of gold grades is accounted for through a set of 25 simulations generated by the sequential Gaussian simulation (SGS) method [32,53,54] for 107,520 mining blocks of size 10 m × 10 m × 10 m (Figure 8a). The set of simulations was generated and properly validated as per the standard practice. The dataset is located from 400 m to 830 m below the processing plant level. Two geotechnical zones (Figure 8b) are delimited by an irregular and inclined separation surface (which provides a more general case than simple distinct horizontal geotechnical zones). The blocks lying above and below this separation surface are flagged accordingly. The cross-sections of Figure 8 emphasise a high-grade region in the top-left portion of the deposit, located in the upper geotechnical zone, and another high-grade region from the centre to the right, in the lower geotechnical zone. Table 5 summarises the information about the input underground gold orebody.

Each geotechnical zone has a specified level spacing, horizontal (sill/crown), rib, and longitudinal pillar sizes, as well as a set of stoping shapes given the conditions of the underlying rock masses (Table 6). The proposed method is used to select the best primary access among three potential shafts. The shafts' headframes are at the same distance from the orebody's footwall, which is the rock mass beneath a steeply dipping deposit [17]. However, Shaft 1 is located at the centre of the deposit's strike (axis y), whereas the other two options are −200 m and +200 m away from Shaft 1. The shafts have the same hoisting capacity, although different capacities and more locations could be used. In each level, the main drifts are developed along the strike. Accordingly, two main mining directions $d \in D_l$ are considered, that is, the northern and southern sides of each shaft option, so as to define the subsets of potential stopes (Figure 4). The overall hoisting, processing and

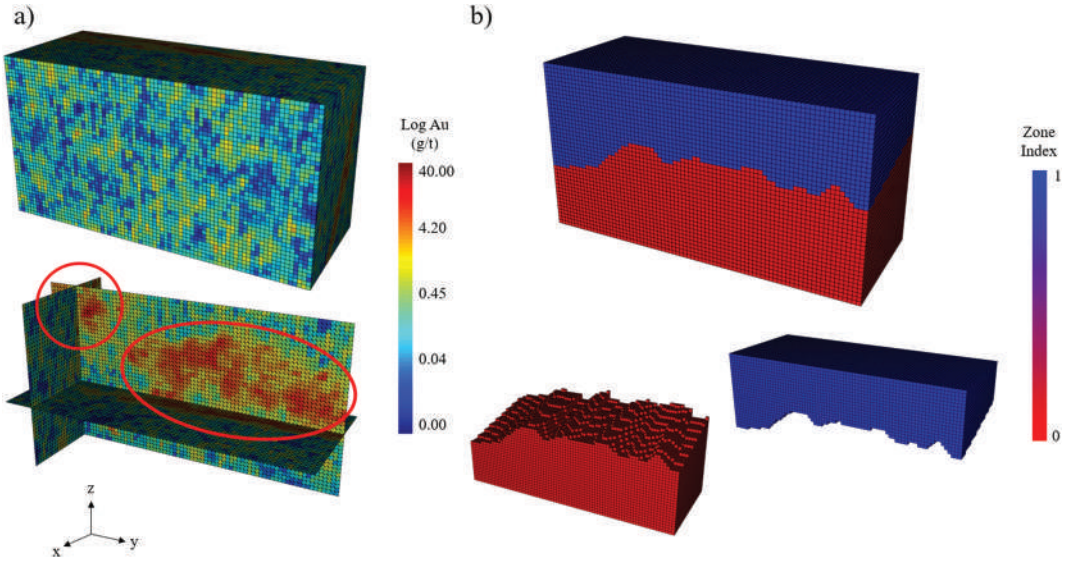

Figure 8. A) One simulated realisation of gold grades of the input underground deposit with a block size of 10 m x 10 m x 10 m, and b) the two input geotechnical zones.

Table 5. Input orebody information.

Parameter	Value/Description
Metal	gold
Grade unit	g/t
Total number of realisations	50
Number of realisations for optimisation	25
Number of realisations for risk analysis	25
Depth from processing plant level (surface)	400 m – 830 m
Dimension along the orebody strike	800 m
Dimension across the orebody strike	320 m
Orientation of strike	Along axis y
Average orebody dip	70°
Number of blocks	107,520
Block size	10 m x 10 m x 10 m

development rate capacities are presented in Table 7 and are obtained by multiplying yearly capacities by the expected number of years of the life-of-mine of the operation. Other economic and technical parameters used in the stochastic stope design optimisation are also presented in this table.

Given the specified level spacing of 40 m and 60 m, respectively, for the upper and lower geotechnical zones, 51 overlapping levels are generated within the two geotechnical zones. The upper and lower zones have, respectively, 12 and 15 set up allowable stoping shapes. During the stope search step, no predefined cut-off grade was used, which means that only the upper part of Eq. 2 is used to determine the economic value of blocks. A probability threshold of 50% is used to exclude negatively valued stopes generating 31,454 potential stopes (with related overlapping information) within the 51 levels during the preprocessing steps of Figure 2. The proposed SIP model is solved using the CPLEX v.12.8.0 software's solver engine [55] implemented with C++ language. This instance has 31,535 binary decision variables and 97,107 constraints. Using a standard personal computer with six cores and 32 GB RAM, the preprocessing and optimisation steps take less than 4 hours to be solved with less than a 1% optimality gap [55–57].

Table 6. Information about the geotechnical zones.

Zone	Parameters	Value
Upper zone	Number of allowable stope shapes	12
	Level spacing	40 m
	Stope heights	20– 40 m
	Stope widths	20– 30 m
	Stope lengths	30– 50 m
	Sill/crown pillar size	10 m
	Rib pillar size	10 m
	Longitudinal pillar size	10 m
Lower zone	Number of allowable stope shapes	15
	Level spacing	60 m
	Stope heights	40– 60 m
	Stope widths	10– 20 m
	Stope lengths	30– 50 m
	Sill/crown pillar size	10 m
	Rib pillar size	10 m
	Longitudinal pillar size	20 m

Table 7. Economic and technical parameters used in the proposed stochastic stope design optimisation of the underground gold mine.

Parameter	Value
Metal price ($/ozt)	1,200
Processing recovery (%)	94%
Mining cost ($/t)	118
Processing cost ($/t)	20
Shaft development cost ($/m) for all $k \in K$	20,000
Drifts development cost ($/m)	7,000
Density (t/m^3)	2.9
Block tonnage (t)	2,900
Overall mining (transportation) capacity (Mt)	4.3
Overall processing capacity (Mt)	4.3
Overall drift development capacity (m)	3,000
Number of shaft options	3
Coordinates of shaft 1 (x, y, z)	123,575, 258,020, 1200
Coordinates of shaft 2 (x, y, z)	123,575, 258,220, 1200
Coordinates of shaft 3 (x, y, z)	123,575, 257,820, 1200
Penalty cost for transportation capacity	1
Penalty cost for development capacity	10
Penalty cost for processing capacity	10
Penalty cost for metal component	0.1

Figure 9a presents the stochastic stope layout obtained by the application of the proposed method at the underground gold mine. The positions of the stope layout and the potential shaft locations with respect to the surface level and the input orebody models are shown in Figure 9b. The layout has six selected production levels satisfying the spacings of 40 m and 60 m for each geotechnical zone, and sill/crown pillar height of at least 10 m. The bottom portion of the lower geotechnical zone (red block edges of Figure 9b) is also mineralised and has positively valued stopes. Nevertheless, these stopes are not profitable so as to compensate for the related incremental shaft and drifts' development cost. Consequently, no stope is selected in this bottom area.

The 46 stopes in the final layout satisfy the allowable minimum and maximum stope sizes and the minimum transversal and rib pillar sizes of each geotechnical zone, as presented in Table 6. The stoping shapes have variable heights and are aligned with the respective production levels' bases. These shapes will be further connected by haulage and drilling drifts and loading crosscuts once the development network is designed. The optimisation process selects the most centralised shaft option (Figure 9b). The profitable stopes of the upper geotechnical zone (blue) are more concentrated towards the negative y-axis direction, and the lower geotechnical zone (red), in turn, has more stopes towards the positive y-axis

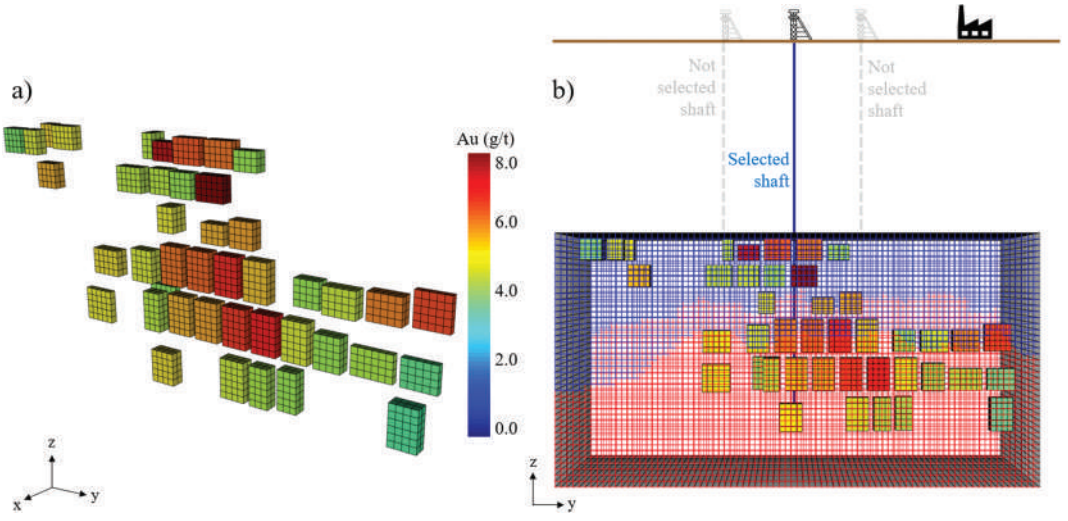

Figure 9. Stochastic stope design: (a) stopes' gold grade, and (b) the locations of the surface level, the stope layout (front view), the selected shaft, and the geotechnical zones.

direction (Figure 9a), which are related to the high-grade lobes circled in Figure 8a. Therefore, the selected shaft balances the associated drifts' development costs. As for the bottom part of the deposit, eventual stoping areas at the periphery of each level are not selected to minimise the final design's drifts development costs. Finally, shaft depth is defined by the deepest selected level, located at 745 m below the surface (Figure 9b).

Table 8 presents the risk analysis of the generated stope layout, which is defined by the non-exceedance probabilities of 10%, 50%, and 90% (P10, P50, P90, respectively) of key performance indicators (KPIs) [58], such as undiscounted profit, recoverable metal, average grade, and total tonnage. A set containing 25 realisations of block's gold grade, different from those used for the stope design optimisation step, is used to generate the risk profiles. The economic potential of the output layout is 217.3 M$, after the deduction of about 30 M$ for the associated shaft and drifts development costs, with a total ore tonnage of 4.6 Mt, 24.1 tons of recoverable metal at an average gold grade of 5.3 g/t, considering the 50^{th} percentile (P50) of the risk profiles.

The penalty costs used in the objective function (Eq. 1) are calibrated by testing different orders of magnitude. The magnitude of the penalty cost associated with the metal reduction component in the objective function expresses the mine planner's tendency to capitalise on the design's upside potential in terms of recovered metal. By increasing the magnitude of such penalty (c^{metal}), more stopes and levels are selected, resulting in physically different designs and related forecasts. Therefore, a mine planner would test different orders of magnitude for all penalty costs and select a final layout based on pertinent mining aspects, on the generated risk profiles and on performance indicators such as undiscounted profit and/or recoverable metal. For the current case study, the scenario having the highest undiscounted profit and metal was selected.

Table 8. Forecasts of the proposed stochastic stope design.

Forecast	P10	P50	P90
Total tonnage (Mt)	4.6	4.6	4.6
Recoverable metal (t Au)	23.8	24.1	24.8
Average gold grade (g/t)	5.2	5.3	5.4
Undiscounted profit (M$)	197.9	217.3	237.1

Table 9. MSO physical parameters.

Parameter	Value/Description
Optimisation method	Slice Method
Optimisation objective	Maximise total value
Stope shape framework	YZ vertical
Level spacing (m)	60 m (along axis z)
Section spacing (m)	40 m (along axis y)
Slice width (m)	10 m (along axis x)
Minimum stope width (m)	10 m (along axis x)
Maximum stope width (m)	30 m (along axis x)
Sill pillar size (m)	10 m (along axis z)
Transversal pillar size (m)	10 m (along axis y)
Longitudinal pillar size (m)	20 m (along axis x)
Fixed stope dip	90°
Fixed stope strike	0° (aligned to axis y)
Number of vertical sub-shapes	3 (sublevels of 20 m high)

3.1. Comparison with a conventional stope design approach

The proposed stochastic stope design optimisation method is compared to the Mineable Shape Optimiser (MSO), an industry-standard automated stope design tool (Alford Mining Systems 2016) 26, and its so-called Slice Method is chosen since it is broadly used in the mining industry for sublevel stoping design. The MSO implements a deterministic approach, requiring an estimated orebody model as an input, which is a smooth representation of the related orebody. An E-type or average model [32,54] is used as the estimated model by averaging the set of 50 block-support gold grade simulated realisations of the deposit.

To attain an equitable comparison between the two approaches, a simplified version of the proposed stochastic stope design optimisation method is used by removing some features of the original approach that the MSO does not consider. First, since MSO defines the stope layout individually for each geotechnical zone based on the fixed levels, sill pillars, and rib pillars, a single geotechnical zone library is defined for the entire deposit for both methods. The original stochastic method would simultaneously select the best set of levels for multiple zones, rather than optimising each zone specifically. Second, the variable stopes' heights and the stopes' lengths along the strike of the stochastic optimisation method were removed. Instead, a fixed stope length (along y) of 40 m and a fixed stope height equal to the level spacing of 60 m are defined to coincide, respectively, with the spacings used by MSO. Capacity constraints and development costs are not considered for the stochastic approach since those components are not incorporated by MSO.

An MSO slice framework oriented along the orebody's strike direction (axis y) is selected, defining a regular grid of stopes' height and length, and the required user-defined sill and transverse pillars' thicknesses and locations. The objective of maximising the total layout's economic value is defined using the same economic parameters, such as metal price, recovery, mining, and processing costs, shown in Table 7. The MSO software tool provides sophisticated stope shape parameters to fit in the orebody's footwall/hang-wall strike and dip. Nonetheless, only cuboid shapes are allowed for a comparison with the proposed method. Orebody control wireframes are not used to provide a pure block value-based stope layout since such contours are also uncertain and are based on subjective geologic interpretations [59,60]. The parameters used on MSO are presented in Table 9.

Figure 10 depicts the comparison between the two generated stope layouts and stresses the stochastic optimisation approach's essential strengths. Since the smooth input estimated model of MSO misrepresents the spatial connectivity and variability of high grades, a more contiguous stope layout is generated (Figure 10b), as compared to the proposed stochastic approach (Figure 10a). MSO is unable to define stoping areas in the border of some levels. The proposed stochastic approach also has the flexibility to allocate profitable levels and rib pillars, which are required inputs for MSO.

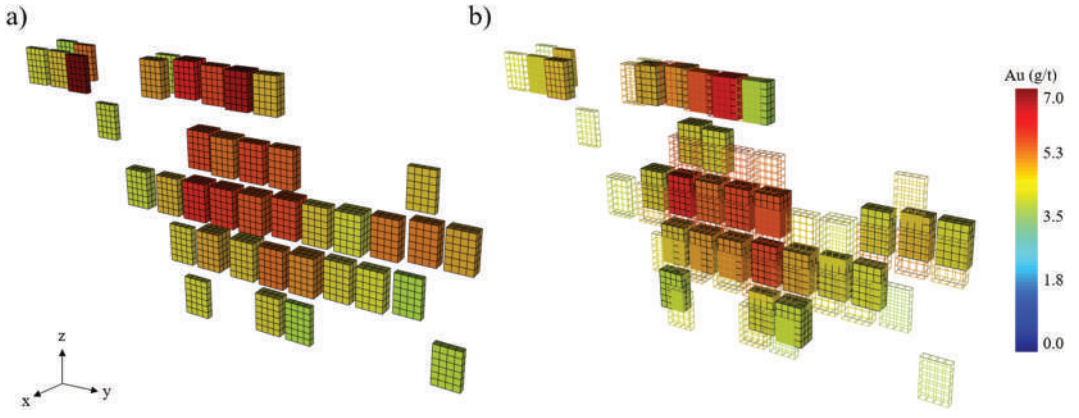

Figure 10. Comparison of stope designs: (a) simplified stochastic approach and (b) slice method of MSO. The unfilled outlines of (b) correspond to the stochastic stope design of (a).

The forecasts of metal tonnage, undiscounted profit, gold grade, and ore tonnage (assuming that all material inside the stopes is ore) of the stope layouts generated by the proposed stochastic method and MSO are presented in Figure 11, where grey dots represent the resultant risk profiles generated by a set of 25 simulations, and the red diamonds represent related 10^{th}, 50^{th}, and 90^{th} percentiles. The black squares represent forecasts generated by MSO. The proposed stochastic method outperforms the MSO (compared to the prompt MSO report), both in terms of recoverable metal and undiscounted profit by 21% and 40%, respectively, highlighting the inherent limits of deterministic stope designs in determining profitable stoping locations and sizes. Moreover, other features of the original stochastic stope design method, such as variable stope length and height, and the integration of development costs and project capacities, are not accounted for by MSO and were not included in the current comparison.

4. Conclusions

A two-stage stochastic integer programming (SIP) model for the stope design optimisation of underground mines employing the sublevel open stoping mining method was proposed. Multiple equiprobable simulated orebody models are used to quantify the grade uncertainty and variability, to provide a risk-resilient stope layout that capitalises on the mineral deposit's upside potential. The proposed mathematical formulation seeks to maximise the undiscounted profit from the selected levels and stopes, while minimising the associated development costs of the shaft and drifts, as well as the economic impacts of exceeding the project's capacities while considering different geomechanics zones. Unlike the conventional stope layout approaches, the proposed approach accounts for uncertainty and variability of grades in the mineral deposit, stopes' accessibility/remoteness, and the capacities that affect stoping sizes, locations, and profitability. A set of possible primary shaft locations, an assortment of potential production levels, stoping sizes and positions, as well as associated distances levels-to-surface and stopes-to-access options are the required inputs for the model. The output of the proposed SIP is a mineable stochastic stope design comprising an optimal combination of horizontal production levels separated by required sill/crown pillar heights, unified stopes with variable height, length, and width satisfying rib and longitudinal pillars requirements, and the best shaft location, which minimises the layout's vertical and horizontal development costs.

The practical aspects of the SIP model were shown in a case study at an underground gold mine. A set of geostatistical simulations of gold grades, three possible shaft headframe locations, two irregularly separated geotechnical zones with defined multiple allowable stoping shapes, level heights, and pillar sizes, and the overall hoisting, processing, and development rate capacities

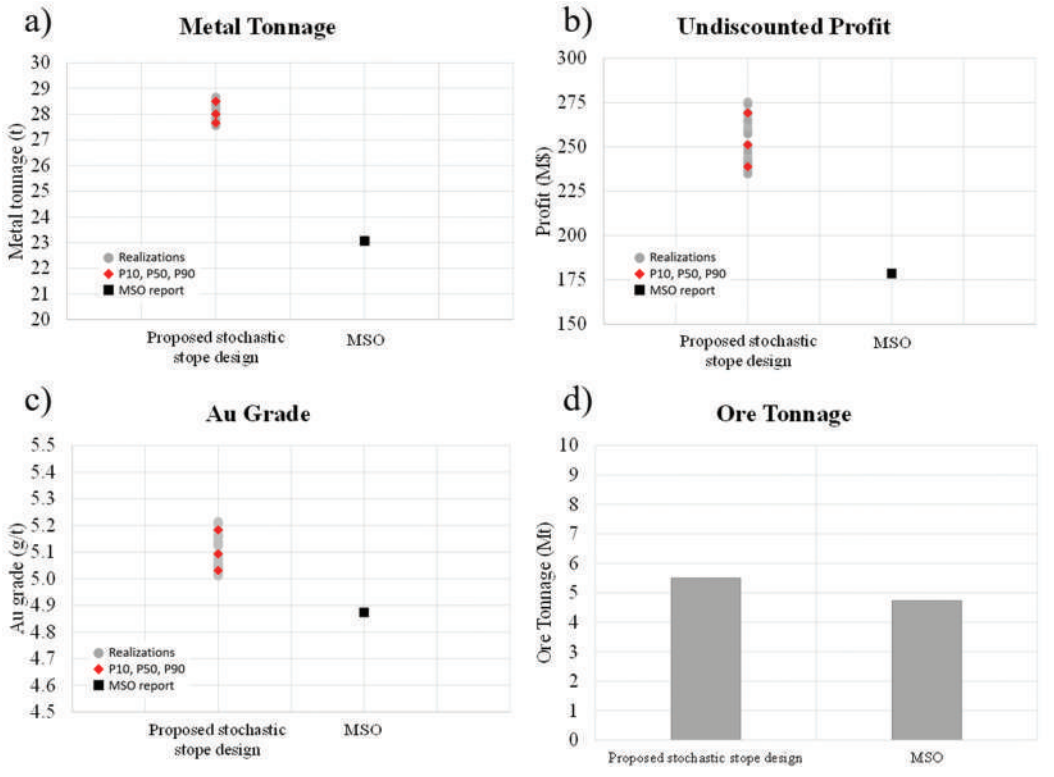

Figure 11. Forecasts stope layouts generated by the proposed stochastic optimisation approach (risk analysis) and by the Slice Method of MSO (report generated by MSO): (a) Metal tonnage, (b) undiscounted profit, (c) average gold grade, and (d) ore tonnage.

were the integrated components of the stope layout optimisation process. A comparison of the proposed method with the Mineable Shape Optimiser (MSO), a deterministic industry-standard automated stope design tool, was performed. The results highlighted two advantages of the proposed approach. First, the incorporation of grade uncertainty into the optimisation process allows one to define some stoping volumes that are not identified by deterministic methods that rely on an estimated orebody model, which mispresents the connectivity of high grades within the deposit. A second advantage is the proposed method's flexibility to define optimal production levels and transverse pillars, which are inputs for MSO. The proposed method produced a layout with significantly higher recoverable metal and undiscounted profits (21% and 40%, respectively). It is worth underlining that, in this comparison, some advanced components of the proposed method, such as incorporating the development costs, variable stopes' lengths along the orebody's strike and heights, and economic impacts of exceeding the project's capacities, were not considered since the conventional stope design approach does not incorporate these aspects.

Further extensions of the current method might implement different metaheuristic solvers to make larger instances tractable and incorporate non-linear components into the optimisation process. The integration of development costs opens new avenues for simultaneous stochastic optimisation of the stope design and the mine production scheduling into a single model. Such an integrated model might be compounded in the optimisation of mining complexes accounting for multiple mines, processing destinations, and marketable products in later developments.

Disclosure statement

No potential conflict of interest was reported by the author(s).

Funding

This work was funded by the Natural Sciences and Engineering Research Council (NSERC) of Canada, CRD Grant CRDPJ 500414-16, the COSMO Mining Industry Consortium (AngloGold Ashanti, BHP, De Beers/ Anglo American, IAMGOLD, Kinross, Newmont and Vale), and NSERC Discovery Grant 239019. Special thanks are to Newmont Corporation and, in particular, Dr. Arja Jewbali for data and collaboration;

ORCID

Roussos Dimitrakopoulos http://orcid.org/0000-0001-7329-2209

References

[1] E. Topal and J. Sens, *A new algorithm for stope boundary optimization*, J. Coal Sci. Eng 16 (2) (2010), pp. 113–119. doi:10.1007/s12404-010-0201-y.
[2] G. Erdogan, M. Cigla, E. Topal, and M. Yavuz, *Implementation and comparison of four stope boundary optimization algorithms in an existing underground mine*, Int. J. Mining, Reclam. Environ 31 (6) (2017), pp. 389–403. doi:10.1080/17480930.2017.1331083.
[3] C. Alford, M. Brazil, and D.H. Lee, *Optimisation in underground mining*, in *Handbook of Operations Research in Natural Resources*, A. Weintraub, C. Romero, T. Bjørndal, R. Epstein, and J. Miranda, eds., Springer, Boston, Massachusetts, USA, 2007, pp. 561–577.
[4] C. Musingwini, Presidential address: optimization in underground mine planning - developments and opportunities, J. South. African Inst. Min. Metall 116 (9) (2016), pp. 809–820. doi:10.17159/2411-9717/2016/v116n9a1.
[5] A.S. Nhleko, T. Tholana, and P.N. Neingo, *A review of underground stope boundary optimization algorithms*, Resour. Policy 56 (July) (2018), pp. 59–69. doi:10.1016/j.resourpol.2017.12.004.
[6] M. Kumral and Y.A. Sari, "Underground mine planning for stope-based methods," in *2nd International Conference on Earth Science, Mineral, and Energy (ICEMINE)*, Yogyakarta, Indonesia, vol. 2245, no. July, pp. 0300141–0300147, 2019.
[7] E. Topal, "Long and short term production scheduling of Kiruna iron ore mine, Kiruna, Sweden, M.Sc. Thesis," Colorado School of Mines, Golden, Colorado, USA, 1998.
[8] E. Topal, "Advanced underground mine scheduling using mixed integer programming, Ph.D. Thesis," Colorado School of Mines, Golden, Colorado, USA, 2003.
[9] M. Vallée, *Mineral resource + engineering, economic and legal feasibility = ore reserve*, CIM Bull 93 (2000), pp. 53–61.
[10] J.-M. Rendu, *Risk Management in Evaluating Mineral Deposits*, Society for Mining, Metallurgy & Exploration, Englewood, Colorado, USA, 2017.
[11] P. Myers, C. Standing, P. Collier, and M. Noppé, *Assessing underground mining potential at Ernest Henry Mine using conditional simulation and stope optimisation*, in *Orebody Modelling and Strategic Mine Planning,* Spectrum Series, Vol. 14, 2nd ed., R. Dimitrakopoulos, ed., Australasian Institute of Mining and Metallurgy, Sydney, NSW, Australia, 2007, pp. 191–200.
[12] R. Dimitrakopoulos and N. Grieco, Stope design and geological uncertainty: quantification of risk in conventional designs and a probabilistic alternative, J. Min. Sci 45 (2) (2009), pp. 152–163. doi:10.1007/s10913-009-0020-y.
[13] A. Jewbali, H. Wang, and C. Johnson, *Resource model uncertainty analysis and stope optimizer (MSO) evaluation for an underground metal mine Project*, in *Application of Computers and Operations Research in the Mineral Industry (APCOM)*, Society for Mining, Metallurgy and Exploration (SME), Fairbanks, Alaska, USA, 2015, pp. 625–640.
[14] O. Tavchandjian, A. Proulx, and M. Anderson, *Application of conditional simulations to capital decisions for Ni-Sulfide and Ni-Laterite deposits*, in *Orebody Modelling and Strategic Mine Planning*, Spectrum Series, Vol. 14, 2nd ed., R. Dimitrakopoulos, ed., Australasian Institute of Mining and Metallurgy, Sydney, NSW, Australia, 2007, pp. 319–333.
[15] W.A. Hustrulid and R.L. Bullock, *Underground Mining Methods: Engineering Fundamentals and International Case Studies*, Society for Mining, Metallurgy and Exploration (SME), Littleton, Colorado, USA, 2001.

[16] E. Villaescusa, *Geotechnical Design for Sublevel Open Stoping*, CRC Press - Taylor & Francis Group, New York, USA, 2014.
[17] H. Hamrin, *Underground mining methods and applications*, in *Underground Mining Methods: Engineering Fundamentals and International Case Studies*, W.A. Hustrulid and R.L. Bullock, eds., Society for Mining, Metallurgy and Exploration (SME), Littleton, Colorado, USA, 2001, pp. 3–14.
[18] R.T. Pakalnis and P.B. Hughes, *Sublevel stoping*, in *SME Mining Engineering Handbook*, P. Darling, ed., 3rd ed., Society for Mining, Metallurgy, and Exploration, Inc, Englewood, Colorado, USA, 2011, pp. 1355–1363.
[19] C. Alford, *Optimisation in underground mine design*, in *Application of Computers and Operations Research in the Mineral Industry (APCOM)*, The Australasian Institute of Mining and Metallurgy, Brisbane, Queensland, Australia, 1995, pp. 213–218.
[20] M. Ataee-Pour, *Optimisation of stope limits using a heuristic approach*, Min. Technol 113 (2) (2004), pp. 123–128. doi:10.1179/037178404225004959.
[21] D.S.S. Sandanayake, E. Topal, and M.W.A. Asad, *A heuristic approach to optimal design of an underground mine stope layout*, Appl. Soft Comput. J 30 (2015), pp. 595–603. doi:10.1016/j.asoc.2015.01.060.
[22] D.S.S. Sandanayake, E. Topal, and M.W.A. Asad, *Designing an optimal stope layout for underground mining based on a heuristic algorithm*, Int. J. Min. Sci. Technol 25 (5) (2015), pp. 767–772. doi:10.1016/j.ijmst.2015.07.011.
[23] M.E. Villalba Matamoros and M. Kumral, *Heuristic stope layout optimisation accounting for variable stope dimensions and dilution management*, Int. J. Min. Miner. Eng 8 (1) (2017), pp. 1. doi:10.1504/IJMME.2017.082680.
[24] V. Nikbin, M. Ataee-pour, K. Shahriar, and Y. Pourrahimian, *A 3D approximate hybrid algorithm for stope boundary optimization*, Comput. Oper. Res 0 (2018), pp. 1–9.
[25] B. Wilson, "Heuristic stochastic stope layout optimization, M.Sc. Thesis," University of Alberta, Edmonton, AB, Canada, 2020.
[26] Alford Mining Systems, "AMS Stope shape optimizer - Reference manual. Version 3.0.0," Alford Mining Systems, Carlton, Victoria, Australia, 3.0.0, 2016.
[27] C. Alford and B. Hall, "Stope optimisation tools for selection of optimum cut-off grade in underground mine design," in *Project Evaluation Conference*, The Australasian Institute of Mining and Metallurgy, Melbourne, Victoria, Australia, pp. 137–144, 2009.
[28] M. Ataee-Pour, *A critical survey of the existing stope layout optimization techniques*, J. Min. Sci 41 (5) (2005), pp. 447–466. doi:10.1007/s10913-006-0008-9.
[29] X. Bai, D. Marcotte, and R. Simon, *Underground stope optimization with network flow method*, Comput. Geosci 52 (2013), pp. 361–371. doi:10.1016/j.cageo.2012.10.019.
[30] B. Ding, C.W. Pelley, and J.J. de Ruiter, *Determining underground stope mineability using dynamic block value assignment approach*, in *Mine Planning and Equipment Selection*, Hardygóra, M., Paszkowska, G., & Sikora, M., eds., CRC Press, Wroclaw, Poland, 2004, pp. 19–26.
[31] J. Hou, C. Xu, P.A. Dowd, and G. Li, *Integrated optimisation of stope boundary and access layout for underground mining operations*, Min. Technol. Trans. Inst. Min. Metall 0 (2019), pp. 1–13.
[32] P. Goovaerts, Geostatistics for natural resources evaluation. New York, USA: Oxford University Press, 1997.
[33] R. Dimitrakopoulos, C.T. Farrelly, and M. Godoy, *Moving forward from traditional optimization: Grade uncertainty and risk effects in open-pit design*, Min. Technol 111 (1) (2002), pp. 82–88. doi:10.1179/mnt.2002.111.1.82.
[34] A. Boucher and R. Dimitrakopoulos, *Block simulation of multiple correlated variables*, Math. Geosci 41 (2) (2009), pp. 215–237. doi:10.1007/s11004-008-9178-0.
[35] N. Grieco and R. Dimitrakopoulos, *Managing grade risk in stope design optimisation: Probabilistic mathematical programming model and application in sublevel stoping*, Min. Technol 116 (2) (2007), pp. 49–57. doi:10.1179/174328607X191038.
[36] M.E. Villalba Matamoros and M. Kumral, *Underground mine planning: Stope layout optimisation under grade uncertainty using genetic algorithms*, Int. J. Mining, Reclam. Environ 0930 (2018), pp. 1–18.
[37] J.R. Birge and F. Louveaux, *Introduction to Stochastic Programming*, 2nd ed., Springer series in operations research and financial engineering, New York, USA, 2011.
[38] S. Ramazan and R. Dimitrakopoulos, *Stochastic optimisation of long-term production scheduling for open pit mines with a new integer programming formulation*, in *Orebody Modeling and Strategic Mine Planning*, Spectrum Series, *Vol. 14*, R. Dimitrakopoulos, ed., The Australasian Institute of Mining and Metallurgy, Melbourne, Victoria, Australia, 2005, pp. 359–365.
[39] S. Ramazan and R. Dimitrakopoulos, *Production scheduling with uncertain supply: A new solution to the open pit mining problem*, Optim. Eng 14 (2) (2013), pp. 361–380. doi:10.1007/s11081-012-9186-2.
[40] L. Montiel and R. Dimitrakopoulos, Optimizing mining complexes with multiple processing and transportation alternatives: an uncertainty-based approach, Eur. J. Oper. Res 247 (1) (2015), pp. 166–178. doi:10.1016/j.ejor.2015.05.002.

[41] R.C. Goodfellow and R. Dimitrakopoulos, *Global optimization of open pit mining complexes with uncertainty*, Appl. Soft Comput. J 40 (2016), pp. 292–304. doi:10.1016/j.asoc.2015.11.038.
[42] M. F. Del Castillo and R. Dimitrakopoulos, "Dynamically optimizing the strategic plan of mining complexes under supply uncertainty," Resour. Policy, vol. 60, 2019, pp. 83–93. doi:10.1016/j.resourpol.2018.11.019.
[43] Z. Saliba and R. Dimitrakopoulos, "Simultaneous stochastic optimization of an open pit gold mine complex with supply and market uncertainty," Min. Technol., vol. 128, no. 4, 2019, pp. 216–229. doi:10.1080/25726668.2019.1626169.
[44] S. Carpentier, M. Gamache, and R. Dimitrakopoulos, "Underground long-term mine production scheduling with integrated geological risk management," Min. Technol., vol. 125, no. 2, 2016, pp. 93–102. doi:10.1179/1743286315y.0000000026.
[45] S. Huang, G. Li, E. Ben-Awuah, B.O. Afum, and N. Hu, A, *stochastic mixed integer programming framework for underground mining production scheduling optimization considering grade uncertainty*, IEEE Access 8 (2020), pp. 24495–24505. doi:10.1109/ACCESS.2020.2970480.
[46] R. Dirkx, V. Kazakidis, and R. Dimitrakopoulos, *Stochastic optimisation of long-term block cave scheduling with hang-up and grade uncertainty*, Int. J. Mining, Reclam. Environ 0930 (2018), pp. 1–18.
[47] R.L. Bullock and W.A. Hustrulid, *Planning the underground mine on the basis of mining method*, in *Underground Mining Methods: Engineering Fundamentals and International Case Studies*, W.A. Hustrulid and R.L. Bullock, eds., Society for Mining, Metallurgy and Exploration (SME), Littleton, Colorado, USA, 2001, pp. 29–48.
[48] Y. Potvin, "Empirical open stope design in Canada, Ph.D. Thesis," University of British Columbia, Vancouver, BC, Canada, 1988.
[49] A. Leite and R. Dimitrakopoulos, *Stochastic optimization of mine production scheduling with uncertain ore/metal/waste supply*, Int. J. Min. Sci. Technol 24 (6) (2014), pp. 755–762. doi:10.1016/j.ijmst.2014.10.004.
[50] L. Trout, *Underground mine production scheduling using mixed integer programming*, in *Application of Computers and Operations Research in the Mineral Industry (APCOM)*, The Australasian Institute of Mining and Metallurgy, Brisbane, Queensland, Australia,1995, pp. 395–400.
[51] A. Brickey, "Underground production scheduling optimization with ventilation constraints, Ph.D. Thesis," Colorado School of Mines, Golden, Colorado, USA, 2015.
[52] J. Benndorf and R. Dimitrakopoulos, Stochastic long-term production scheduling of iron ore deposits: integrating joint multi-elements geological uncertainty, J. Min. Sci 49 (1) (2013), pp. 68–81. doi:10.1134/S1062739149010097.
[53] N. Remy, B. Alexandre, and J. Wu, *Applied Geostatistics with SGems: A User's Guide*, Cambridge University Press, Cambrigde, United Kingdom, 2009.
[54] C.V. Deutsch and A.G. Journel, *GSLIB: Geostatistical software library and user's guide, 2nd ed., Oxford University Press, New York, USA, 1997.* .
[55] IBM ILOG, "CPLEX user's manual," IBM, p. 596, 2017.
[56] L.A. Wolsey, *Integer Programming*, 2nd ed., John Wiley & Sons, Inc., Hoboken, New Jersey, USA, 2021.
[57] A. Atamtürk and M.W.P. Savelsbergh, *Integer-programming software systems*, Ann. Oper. Res 140 (1) (2005), pp. 67–124. doi:10.1007/s10479-005-3968-2.
[58] P.J. Ravenscroft, *Risk analysis for mine scheduling by conditional simulation*, Trans. Inst. Min. Metall Sect A 101 (1992), pp. A105–A108.
[59] V. Osterholt and R. Dimitrakopoulos, *Simulation of orebody geology with multiple-point geostatistics - Application at Yandi Channel iron ore deposit, WA, and implications for resource uncertainty*, in *Orebody Modelling and Strategic Mine Planning*, Spectrum Series, Vol. 14, 2nd ed., R. Dimitrakopoulos, ed., The Australasian Institute of Mining and Metallurgy, Sydney, NSW, Australia, 2007, pp. 51–60.
[60] G. Bárdossy and J. Fodor, *Traditional and new ways to handle uncertainty in geology*, Nat. Resour. Res 10 (3) (2001), pp. 179–187. doi:10.1023/A:1012513107364.